

B. Bazylev, I. Landman, S. Pestchanyi, R. Fetzner, Yu. Igitkhanov, R.A.Pitts, S. Putvinski, G. Arnoux, S. Brezinsek, A. Huber, M. Lehnen, N. Hartmann, J.W. Coenen, G. Saibene, P. C. Stangeby and JET EFDA contributors

# Modelling of Material Damage and High Energy Impacts on Tokamak PFCs during Transient Loads



# Modelling of Material Damage and High Energy Impacts on Tokamak PFCs during Transient Loads

B. Bazylev<sup>1</sup>, I. Landman<sup>1</sup>, S. Pestchanyi<sup>1</sup>, R. Fetzer<sup>1</sup>, Yu. Igitkhanov<sup>1</sup>, R.A.Pitts<sup>2</sup>, S. Putvinski<sup>2</sup>, G. Arnoux<sup>3</sup>, S. Brezinsek<sup>4</sup>, A. Huber<sup>4</sup>, M. Lehnen<sup>4</sup>, N. Hartmann<sup>4</sup>, J.W. Coenen<sup>4</sup>, G. Saibene<sup>5</sup>, P. C. Stangeby<sup>6</sup> and JET EFDA contributors\*

*JET-EFDA, Culham Science Centre, OX14 3DB, Abingdon, UK*

<sup>1</sup>*Karlsruhe Institute of Technology, IHM, P.O. Box 3640, 76021 Karlsruhe, Germany*

<sup>2</sup>*ITER Organization, Route de Vinon sur Verdon, 13115 Saint Paul Lez Durance, France*

<sup>3</sup>*EURATOM-CCFE Fusion Association, Culham Science Centre, OX14 3DB, Abingdon, OXON, UK*

<sup>4</sup>*Institute of Energy and Climate Research – Plasma Physics, Forschungszentrum Jülich EURATOM-FZJ, Partner of Trilateral Euregio Cluster, 52425 Jülich, Germany*

<sup>5</sup>*Fusion for Energy Joint Undertaking, Josep Pla no. 2 - Torres Diagonal Litoral Edificio B3 7/03 Barcelona 08019, Spain*

<sup>6</sup>*University of Toronto Institute for Aerospace Studies, Toronto, M3H 5T6, Canada*

*\* See annex of F. Romanelli et al, "Overview of JET Results", (24th IAEA Fusion Energy Conference, San Diego, USA (2012)).*

Preprint of Paper to be submitted for publication in Proceedings of the  
24th IAEA Fusion Energy Conference (FEC2012), San Diego, USA  
8th October 2012 - 13th October 2012

“This document is intended for publication in the open literature. It is made available on the understanding that it may not be further circulated and extracts or references may not be published prior to publication of the original when applicable, or without the consent of the Publications Officer, EFDA, Culham Science Centre, Abingdon, Oxon, OX14 3DB, UK.”

“Enquiries about Copyright and reproduction should be addressed to the Publications Officer, EFDA, Culham Science Centre, Abingdon, Oxon, OX14 3DB, UK.”

The contents of this preprint and all other JET EFDA Preprints and Conference Papers are available to view online free at [www.iop.org/Jet](http://www.iop.org/Jet). This site has full search facilities and e-mail alert options. The diagrams contained within the PDFs on this site are hyperlinked from the year 1996 onwards.

## ABSTRACT

A tungsten (divertor) and beryllium (first wall) will be the plasma-facing components used in the nuclear phases of ITER operation. In reactor-scale tokamaks using metallic PFCs, transient events such as ELMs, VDEs and disruptions will produce strong vaporization and surface melting. Likewise, intense heat loads due to the impact of runaway electrons (RE) generated during the current quench phase of disruptions become a major issue in devices operating at high plasma current. Even if the thermal quench energy of major disruptions is expected to be successfully dissipated by mitigation using massive gas injection (MGI), the resulting photonic radiation loads on the ITER Be wall can be very intense. Unfortunately, no existing tokamak or laboratory device can simultaneously match all the conditions of ITER transients and so estimates of expected damage to ITER PFCs can only be provided by numerical simulations, supported by benchmarking on existing experiments. This paper describes a series of applications of the codes MEMOS, ENDEP and TOKES, developed at the Karlsruhe Institute of Technology, to specific ITER transient loading on both W and Be surfaces in the case of W divertor PFC melting due to disruptions (MEMOS), RE impact on Be first wall panels (MEMOS and ENDEP) and estimates of MGI driven photon radiation flash first wall heating (TOKES). An account is also given of benchmarking studies of W damage caused by  $\mathbf{J \times B}$  forces and RE interactions with first wall in which these codes have been compared with results obtained on the JET and TEXTOR tokamaks.

## 1. INTRODUCTION

Tungsten (W) is planned in the nuclear phases (and even now possibly from the beginning of non-active operations) as the armour material for plasma-facing components (PFC) in the ITER divertor [1] and as the main PFC material of future tokamak reactors. Beryllium (Be) will be used as first wall (FW) plasma-facing material on ITER [1] and is currently being used on the FW in the new JET ITER-like Wall (ILW) configuration [2]. Uncontrolled off-normal and transient events, such as ELMs (Edge Localized Modes), VDEs (Vertical Displacement Events) and disruptions on ITER have the potential to drive significant erosion of PFC surfaces by vaporization and melting [3,5]. In particular, melt motion followed by melt splashing of metallic armour components can be very serious, leading to deterioration of PFC surface topology (and possible consequences for subsequent plasma operation), a decrease in PFC lifetime and production of Be and W dust in the form of resolidified droplets.

Scaling from today's experiments to ITER predicts [3-5] that due to the high thermal energy of the confined burning plasma ( $>0.3\text{GJ}$ ), uncontrolled transient heat fluxes on PFCs could reach values in the following range: I) Divertor target: Type I ELMs:  $0.5\text{--}4\text{ MJ/m}^2$  on the timescale of  $0.3\text{--}0.6\text{ms}$ ; disruption thermal quench (TQ):  $2\text{--}25\text{ MJ/m}^2$  ( $1\text{--}5\text{ms}$ ). II) FW: Type I ELMs  $0.5\text{--}2\text{MJ/m}^2$  ( $0.3\text{--}0.6\text{ms}$ ); TQ: up to  $13\text{MJ/m}^2$  for major disruptions and up to  $30\text{ MJ/m}^2$  for upward and downward VDEs (few ms). During disruptions mitigated with massive gas injection (MGI), photon fluxes in the range  $0.1\text{--}2\text{MJ/m}^2$  ( $2\text{--}5\text{ms}$ ) can be deposited on the FW. The runaway electron (RE) fluxes which are expected to be generated during the current quench (CQ) of mitigated and unmitigated

disruptions can be in the range of 20–300 MJ depending on the amount of magnetic energy which can be transferred to RE kinetic energy during CQ with time duration being in the range of 1–100ms for slow loss and in the range up to 10 $\mu$ s for fast loss. The anticipated impact of these powerful ITER transients cannot be reproduced in existing tokamaks. Alternative devices, such as plasma guns (QSPA-T, QSPA-kh50, etc), are thus used for armour testing under extreme conditions. However, the heat pulses created in these facilities cannot simultaneously match all characteristics of ITER transients and estimates of the damage to be expected on ITER must be supported by numerical simulations, benchmarked against experiment. This paper describes a number of such studies, together with a selection of ITER-specific calculations.

## **2. MELT MOTION DAMAGE MODELING BY THE CODE MEMOS**

The 2D version of the melt motion code MEMOS [6] has been earlier benchmarked against melting experiments on the plasma guns for ELM-like heat loads (QSPA-T, QSPA-Kh50) [6] and on the TEXTOR tokamak for steady state like heat fluxes of longer duration [7]. An upgraded, 3D version of the code MEMOS is now available for motion dynamics of a viscous melt. In tokamaks, where strong magnetic fields are present, the melt fluid acceleration can be due to surface tension, applied plasma pressure and the  $\mathbf{J}\times\mathbf{B}$  force of halo-, eddy-, and thermo-currents. The 3D MEMOS code has been recently validated against TEXTOR experiments for long timescale (second) melt motion displacements [8]. Simulated  $\mathbf{J}\times\mathbf{B}$  driven melt motion induced by thermo-currents is in a good agreement with the measurements of target erosion profile produced by the melt displacements. 3D simulations of melt motion damage of JET Be tiles [9] have demonstrated the importance of the  $\mathbf{J}\times\mathbf{B}$  force driven by halo currents for the events on the VDE timescale. Simulation results are in qualitative agreement with the Be tile damage observed in JET. The effects of VDE transients in some specific ITER situations, where the melt layer can exist up to several tens of ms, have also been analysed [10].

## **3. MODELLING OF THE IMPACT OF RE ON A SINGLE BE TILE ON THE JET ITER-LIKE WALL AND ON A SINGLE BE TILE OF THE ITER FIRST WALL.**

A critical issue for ITER, which operates at high plasma current, is the generation of high energy RE beams during disruptions (both natural and MGI mitigated events). Interaction of these intense electron beams with the metallic armour can cause melting and then melt layer acceleration with melt splashing. Numerical simulations of PFC damage due to RE impact are being performed with MEMOS for both JET and ITER. At JET- with CFC walls (JET-C), previously work focused on benchmarking MEMOS and the energy deposition Monte-Carlo code ENDEP [11] using experiments on RE beam interaction with CFC armour tiles [11]. A reasonable quantitative agreement between numerical simulations and experiments has been obtained. Validation of the ENDEP and MEMOS codes performed against TEXTOR experiments on RE interactions with a graphite limiter has also demonstrated reasonable quantitative agreement between the simulations and experiment. New experiments with a Be first wall are currently underway at JET and are being used to validate the

codes taking into account the 3D structure of the Be tiles. Predictive simulations of the RE impact on a single typical Be tile (Fig. 1) aim at the estimation of critical RE current densities causing melting have been performed [8]. These studies are essential for validation of the application of the same codes to study the RE damage of ITER FW, an exercise which is underway and which also takes into account the full 3D structure of the ITER FW panels. In the ITER case, modelling of the after effects of RE beam interaction with typical Be FW panel tiles (Fig. 2) is being performed for fast (with a timescale of 5-20 $\mu$ s) RE events and accounting for the full 3D structure of the ITER FW panel geometry. The castellated Be tiles installed in JET-ILW have a roof-like shape in the toroidal direction, similar to the global first wall panel shaping philosophy employed at ITER, but with large differences in scale size and with the important distinction that the ITER panels are actively water cooled in comparison with inertially cooled JET-ILW components.

Simulations of RE impact onto single Be tiles/wall panels in JET and ITER are subdivided into two steps. In the first, volumetric energy deposition functions are calculated using ENDEP. In the second, the code MEMOS [6] is used to compute temperature distributions inside the Be, taking into account temperature-dependent thermo-physical properties. Typical parameters of RE used in these predictive simulations for JET-ILW are based on the data measured during the JET-C experiments with CFC FW [12]: typical RE current is up to 0.5 MA, beam radius of about 0.5m, (current density up to 0.6MA/m<sup>2</sup>), heat deposition time several ms. It is not thought that RE parameters, if RE do appear during ILW experiments will be much different from the those experienced with dominant carbon PFCs. A total wetted area of 0.6m<sup>2</sup> is expected.

The simulations for both JET and ITER assume RE with exponentially decaying energy distribution functions:  $f(E) \sim \exp(-E/E_0)$ . It is further assumed that the incident electrons move along the toroidal magnetic field lines, rotating with the gyro frequency. Thus, the incident angle of the electrons strongly depends on the gyro parameter and magnetic field direction ( $B = 3.0$ T for JET and  $B = 5.0$  T for ITER). The gyro-radius is determined by the electron kinetic energy,  $E_{tr}$  across the magnetic field  $\mathbf{B}$  and can be defined through the ratio  $\gamma = E_{tr}/E$  where  $E$  is total electron kinetic energy. The inclination angle of the toroidal magnetic field lines with respect to the target surface is  $\alpha \sim 3^\circ$  (JET-ILW) and  $\alpha \sim 1^\circ$  (ITER). Several simulations were carried out for  $E_{tr}/E = 0$  (electrons move along magnetic field lines without gyro motion), and  $E_{tr}/E = 0.02$  with variation of the exponentially decaying RE distribution  $E_0$ : 3, 5, 8MeV (JET-ILW) and  $E_0 = 12.5$ MeV (ITER). Simulations are in addition performed for varying width, L of wetted area along the tile surface: L=1cm and 0.5cm for JET-ILW, L=5cm, 3cm and 1cm for ITER. In the JET-ILW case, parametric MEMOS simulations are performed for scenarios with rectangular pulse shape with duration  $\tau = 1-4$ ms and varying RE beam heat fluxes in the range 0.5–6 MW/cm<sup>2</sup>. As mentioned above, for the ITER case MEMOS simulations thus far have been performed only for scenarios corresponding to fast RE loss, assuming rectangular pulse shape and reference duration  $\tau = 10\mu$ s for different RE beam heat flux densities in the range 100–600MW/cm<sup>2</sup>.

**JET-ILW:** in the case of  $E_{tr}/E = 0$  with L = 1 cm, about 40% of impacting electrons pass through the tile with generation of secondary electrons, which can escape of primary and secondary electrons

from the target. The RE current density drops by 35%. As the ratio  $E_{tr}/E$  increases, more electrons pass through the tile and, for case  $E_{tr}/E = 0.02$ , <40% of the impact energy is absorbed in the tile. A reduction of the wetted area by a factor 2 ( $L = 0.5\text{cm}$ ) leads to a decrease of absorbed energy and an increase of the number of runaway electrons passing through the tile. The efficiency of X-ray generation in all simulated scenarios is rather low (and only  $\sim 0.4\%$  of the impacting energy is re-radiated by Bremsstrahlung). The MEMOS simulations demonstrate that the melting threshold of the RE beam current density depends on the pulse duration as  $1/\tau$  (Fig.3). The calculated melting threshold (ranging between 2 and 12  $\text{kA/m}^2$ ) is much less than the maximum expected RE current density on JET-C, which may reach values up to  $500\text{kA/m}^2$  [12]. A small increase (by 10-20%) of the RE current density above the melting threshold results in Be melting of up to several hundred microns depth with rather long re-solidification time ( $>20\text{ms}$ , see Fig.4). So far no RE beam like in JET-C has been observed with JET-ILW, but MEMOS predict that already currents of 10kA could lead to massive melting of upper dump plate with the melt layer thickness of 500mm.

**ITER:** for all scenarios investigated thus far, the impacting REs do not penetrate deeply into the Be tiles of the FW panels - the absorbed energy distribution stretches in the direction of the RE beam (Fig.5). At depths  $< 2\text{mm}$  the normalized energy distribution profile falls by a factor of 2 (Fig.6), indicating that for these particular RE parameters, the cooling system, which is located at depths  $> 0.8\text{cm}$  from the surface, will not be significantly heated by RE electrons.

For cases with wetted area  $L = 1\text{cm}$ , about 60% of the impacting energy passes through the tile, carried by escaping primary and secondary electrons. The RE current density drops by only  $\sim 20\%$ . When  $L = 3\text{cm}$  ( $5\text{cm}$ ), about 40% (<40%) of the incident RE energy passes through the tile and the RE current density drops by 30% (30-35%).

As in the case of JET, the ENDEP simulations demonstrate that more electrons pass through the ITER tile as  $E_{tr}/E$  increases. A reduction of the wetted area leads to a decrease of absorbed energy and an increase in the number of electrons passing through the tile. Similar also to the JET case, the efficiency of X-ray generation in all simulated scenarios is rather low due to low Z tile material and only  $\sim 1\%$  of the impacting energy is re-radiated by bremsstrahlung. The photons are mostly generated in the spectral region 0.1-2MeV.

The MEMOS simulations demonstrate that the melt threshold depends strongly on the wetted area and  $E_{tr}/E$  (Fig.7). The calculated melting threshold corresponds to RE beam current densities between 250 and 480  $\text{kA/m}^2$  (giving heat loads 300-600  $\text{MW/cm}^2$ ). In common with the findings for JET, the dependence of the melt threshold on RE beam current density and heat flux density of RE beams is sensitive to pulse duration according  $1/\tau$ . For ITER a small increase of the RE beam current density above the melt threshold by 10-20% results in Be melting of up to several hundred mm with rather long re-solidification time ( $>10\text{ms}$ ).

#### 4. TOKES SIMULATIONS OF MASSIVE GAS INJECTION (MGI)

Disruption mitigation experiments MGI on current tokamaks (see e.g. [13]) have demonstrated effective ionization of injected atoms (Ne, Ar, He), the propagation of a cooling wave from the

periphery to the plasma centre, subsequent MHD activity leading to a thermal quench (TQ) within a few ms once the cooling front reaches the magnetic surface at safety factor  $q = 2$  and a photon radiation flash. On the short timescale of the impurity atom ionization, plasma parameters vary strongly in the poloidal direction in the vicinity of the injection leading, for example to drastic decrease in the electron temperature,  $T_e$  near the gas jet, which in turn significantly decreases the ionization rate there, resulting in deep jet penetration.

In 2011-2012 modelling with the tokamak code TOKES [14] has been focused on further development and validation of the MGI process on data from JET, aiming at predictive simulations for ITER. Plasma transport is calculated in both the confined and open field line regions, assuming toroidal symmetry and a fixed magnetic equilibrium throughout the gas jet penetration and up to the thermal quench. The TOKES 2D multi-fluid plasma model is coupled to a radiation model and includes non-equilibrium expansion of ions along magnetic field lines and thermal cross-field transport. In the real experiment, core instabilities develop during the mitigation, deteriorating toroidal symmetry and causing slight overlapping of nested magnetic surfaces, which drastically increases electron cross-transport along ergodized magnetic field lines. After start of cooling plasma periphery moderate instabilities develop at many rational values of  $q$  in the core, rising drastically once the cooling front crosses the  $q = 2$  surface. This is modelled in TOKES by imposing an adhoc increase in the electron cross-field thermal transport at the TQ.

Code simulations have previously been compared with experimental results from Ar MGI into a DIII-D H-mode plasma and recently with Ar MGI into two JET discharges [15], comprising an ohmic pulse (Pulse No: 76314) with total plasma energy content (at the mitigation)  $W = 0.8\text{MJ}$  and an additionally heated H-mode pulse (Pulse No: 77806) with  $W = 3.2\text{MJ}$ . The injected gas is ionized and Ar ions with  $T_i = 100\text{--}50\text{eV}$  expand with velocity  $\sim 50\text{km/s}$ , making one toroidal turn within  $\sim 0.5\text{ms}$ , providing rapid toroidal symmetry. Figure 8 compares simulated and experimental electron temperatures and total radiated power, demonstrating that the code satisfactorily reproduces the main processes occurring during the TQ. TOKES has been used to study the MGI photon flash and subsequent heat loading on the Be wall for a neon MGI case in which injection is made into the baseline burning plasma equilibrium ( $Q = 10$ ,  $W \sim 400\text{MJ}$ ) using simulated core plasma profiles and injection through an upper lateral port as foreseen for the ITER MGI systems [16]. The aim of these studies is to investigate the potential for MGI to drive melting over the large Be wall surface area in ITER as a result of the mitigation flash. The output of the TOKES simulations is used by MEMOS to assess the maximum wall surface temperature, assuming an initial (pre-disruptive) uniform wall temperature of  $T_0 = 500\text{K}$ .

Being 2D, the TOKES code cannot simulate the toroidally discrete gas injection. Instead, a single injection orifice is modelled as a gap in the FW contour, uniformly distributed toroidally, such that the gas injection is toroidally symmetric in the code.

The necessity to outpace the dump of disruptive plasma energy limits the acceptable cooling time,  $\tau_c$  to a few ms (and thus the TQ stage duration;  $\tau_c$  is the whole cooling time from the valve opening time at  $t = 0$ ). In the studies performed thus far for Ne, the strategy has been to seek an

optimum amount of injected Ne with  $\tau_c$  as short as possible, provided the maximum temperature on the Be surface,  $T_{w,max}$  does not exceed the Be melting point,  $T_{melt} = 1564K$ . For this purpose MGI scenarios are examined with respect to  $T_{w,max}$  by varying the initial pressure in the injector gas plenum.

As an example, Fig.9 shows radial  $T_e$  profiles for the maximum gas inflow considered,  $J_m = 2.6 \times 10^{26}$  atom/s, plotted as a function of radial distance from the magnetic axis at the outboard midplane. Very rapidly after the injection, the dependence  $T_e(r,t)$  acquires the feature of a cooling wave propagating from the periphery to the plasma centre.

The simulations reveal an important difference between cases with  $J_m < J_{m0} \approx 2 \times 10^{26}/s$  and  $J_m \geq J_{m0}$ . Figure 10 shows the poloidal distribution of the wall surface temperature for four cases with varying  $J_e$ . In the case of the highest  $J_m$  the cooling time is very rapid ( $\tau_c = 3.4ms$ ) and the ionized  $N_2$  has insufficient time to leave the injector location at the wall coordinate  $\approx 14.5m$ . In the low inflow case ( $J_m = 0.65 \times 10^{26}/s$ ) the cooling time is longer (7.8ms) giving the ionized gas more time to expand along the magnetic field lines. This decreases the load in front of injector.

The case of  $J_m = 1.3 \times 10^{26}/s$  has the shortest cooling phase of the three MGI examples studied ( $\tau_c = 5.7ms$ ) and produces no melting anywhere on the FW. This implies an injector plenum pressure  $\approx 50$  bar. Of the cases studied, it is also the one in which the radiation energy is deposited most uniformly over the FW.

Figure 11 shows both the injected neon mass  $M_{inj}$  in the vessel and the calculated mixing efficiency (assimilation)  $m = M_{ion}/M_{inj}$ , where  $M_{ion}$  is the mass of ionized Ne;  $m$  decreases monotonically with  $J_m$ . The low values of  $m$  mean that the majority of the Ne reaching the vacuum vessel remains as neutrals. Only the atoms which have been ionized radiate at the jet front, with the large fraction of the injected neon remaining in the injected cloud behind the cooling wave.

## CONCLUSIONS

Predictive numerical simulations of RE impact onto typical JET and ITER Be tiles have been performed with the Monte Carlo code ENDEP and the code MEMOS aiming estimations of after effect of RE impact. The current densities of RE beam which cause melting of Be tiles (melting thresholds) are determined for different potential scenarios of RE heat loads. Small increase of RE beam current density above the melting threshold by 10–20% results in the Be melting up to several hundred microns with rather long re-solidification time ( $>20ms$ ). Simulations demonstrate that cooling system, disposed at the deepness of 0.8cm from the surface, will not be significantly heated or damaged by RE beams. Further comprehensive 2D and 3D ENDEP and MEMOS simulations will be carried out to predict melt damage to Be plates for different scenarios expected in ITER for fast and slow RE impacts.

Simulations using the codes TOKES and MEMOS have been performed to study numerically MGI in JET and to act as a validation step for the prediction of the photonic heating of the ITER Be FW in the case of MGI applied to high stored energy burning plasmas. For example, for an initial gas injector plenum pressure of 30 bar and gas inflow rate of  $1.3 \times 10^{26}$  atom/s (corresponding to

20 g of injected Ne), complete plasma cooling occurs on a timescale of 5.7 ms with a maximum wall surface temperature at the thermal quench of  $\sim 1400$  K and avoiding Be melting at any point on the first wall. For more intense injection (with cooling time  $< 5$  ms), the photon radiation load is highest in front of the injector location, resulting in surface temperatures exceeding Be melting. One important shortcoming of these simulations is the 2D nature of TOKES, which cannot reproduce the toroidally discrete nature of the injection in the real situation. However, this 3D effect may be much less pronounced than might be thought owing to the rapid longitudinal expansion of plasma along field lines and the thermal energy density in the peripheral plasma much lower than that in the core. Further studies are planned to examine this possibility more closely.

## ACKNOWLEDGEMENTS

This work, supported by the European Communities under the EFDA Task Agreement between EURATOM and Karlsruhe Institute of Technology (KIT) and by F4E grant G-315 for KIT, was carried out within the framework of the European Fusion Development Agreement. The views and opinions expressed herein do not necessarily reflect those of the European Commission.

## REFERENCES

- [1]. Pitts R.A. et al., “A Full Tungsten Divertor for ITER: Physics Issues and Design Status”, 20<sup>th</sup> International Conference on Plasma Surface Interaction in Controlled Fusion Devices (PSI) (2012) Aachen, Germany, Journal of Nuclear Materials in press
- [2]. Matthews G. et al., “Plasma operation with metallic wall: direct comparison with all carbon environments”, 20<sup>th</sup> PSI (2012) Aachen, Germany, Journal of Nuclear Materials in press
- [3]. Federici, G., et al, Plasma Physics and Controlled Fusion **45** (2003) 1523
- [4]. Mitteau R. et al., Physica Scripta **T145** (2011) 014081
- [5]. Loarte A., et al., Physica Scripta **T128** (2007) 222
- [6]. Bazylev B, et al., Journal of Nuclear Materials (2009) **390-391**, pp. 810-813
- [7]. Bazylev B, et al., Physica Scripta **T145** (2011) 014054,
- [8]. Bazylev B, Coenen J.W, Pitts R.A, Philipps V, “Modeling of Tungsten Armour Damage under ITER-like Transient Heat Loads”, 15<sup>th</sup> International Symposium on Flow Visualization. (2012) Minsk, Belarus.
- [9]. Bazylev B, et al., “Modeling of the Impact of Runaway Electrons on the ILW in JET”, 20<sup>th</sup> PSI (2012) Aachen, Germany to be published in Journal of Nuclear Materials.
- [10]. Bazylev B, Landman I, Pitts R.A, Simulations of Transient Heat Flux Damage on Leading Edges in the ITER All-Tungsten Divertor, ICFRM-15 (2011) Charleston, USA in press, to be published in Journal of Nuclear Materials.
- [11]. Bazylev B, et al., Journal of Nuclear Materials **415** (2011) S841.
- [12]. Lehnen M, et al. Journal of Nuclear Materials **390-391** (2009) 740-746.
- [13]. Lehnen M, et al., Nuclear Fusion **51** (2011) 123010.

- [14]. Landman I, et al Fusion Engineering and Design **86** (2011) 1616-1619
- [15]. Pestchanyi S, et al, Fusion Engineering and Design (2012) doi: 10.1016/j.fusengdes.2012.02.107.
- [16]. Maruyama et al., “ITER Fuelling and Glow Discharge Cleaning System Overview”, 24<sup>th</sup> IAEA FEC conference, San Diego 8-13 October 2012 - paper ITR/P5-24.

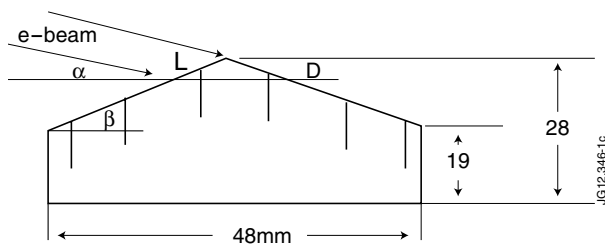


Figure 1: Geometry of a typical Be upper dump tile in the JET ILW.

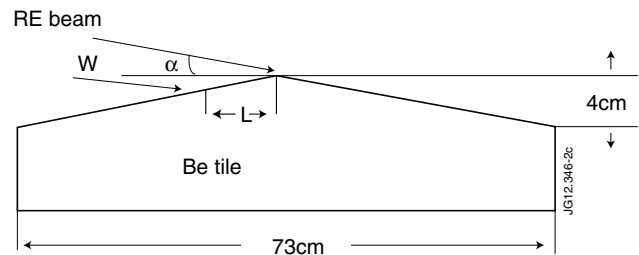


Figure 2: Geometry of typical Be tiles corresponding to a single wing of an ITER FW panel module.

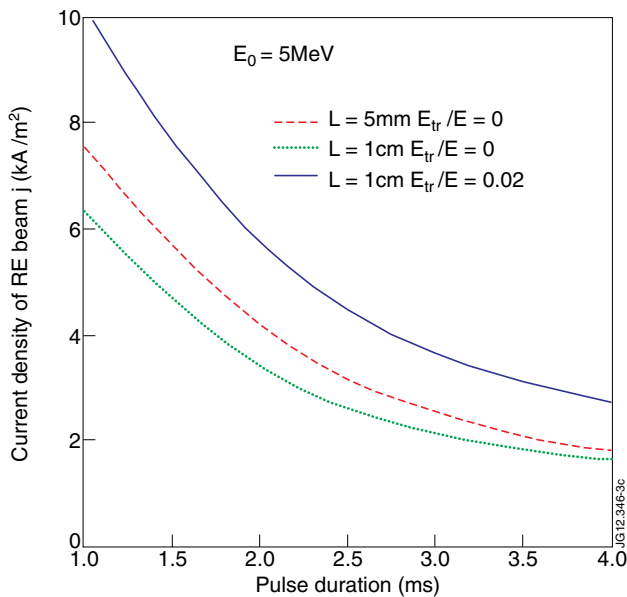


Figure 3: Dependence of RE current density on heat pulse duration corresponding to the melting threshold for scenarios with  $E_0 = 5\text{MeV}$  (JET).

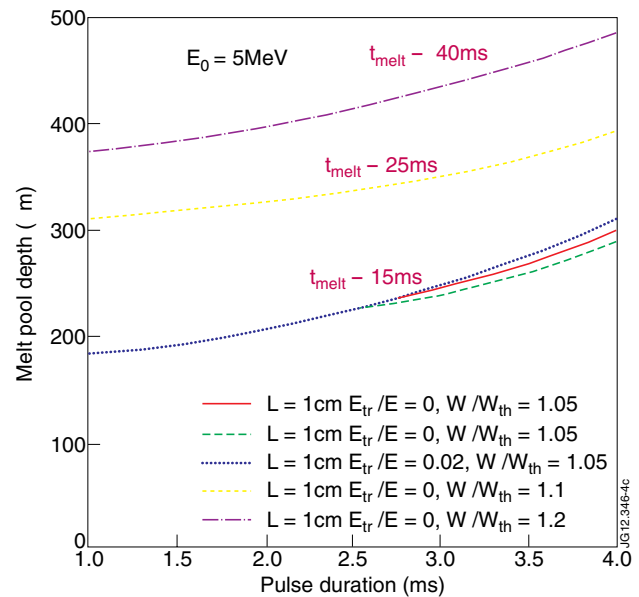


Figure 4: Dependence of the maximum of melt pool depth on pulse duration for scenarios with  $E_0 = 5\text{MeV}$  and different heat loads exceeding the melting threshold,  $W_{th}$  (JET).

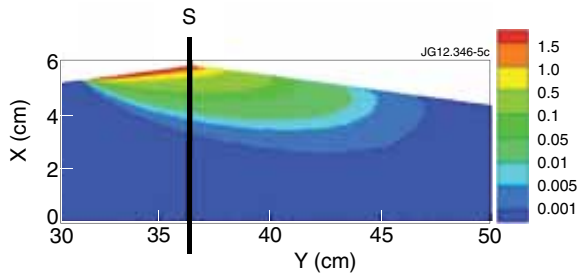


Figure 5: Normalized function of absorbed energy inside the simulated region of an ITER FW panel (wetted area along toroidal surface  $L = 5\text{cm}$ ,  $E_{tr}/E = 0$ ).

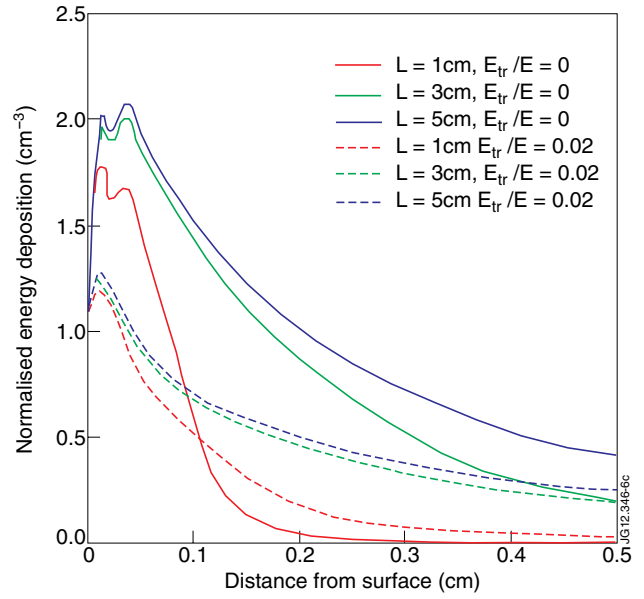


Figure 6: Normalized profiles of absorbed energy inside the ITER Be FW panel along the vertical line (see Fig.5) for different scenarios of impacting REs.

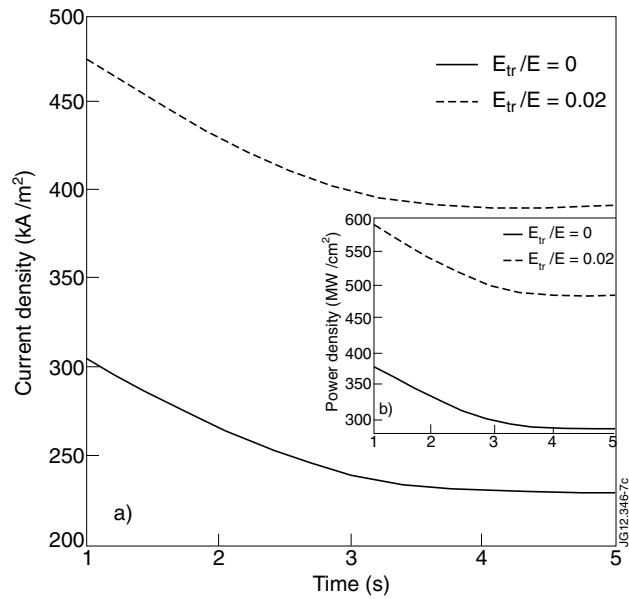


Figure 7: Dependence of current density (a) and power density (b) of the RE beam corresponding to the melting threshold on the wetted area along the ITER Be FW panel for varying  $E_{tr}/E$ .

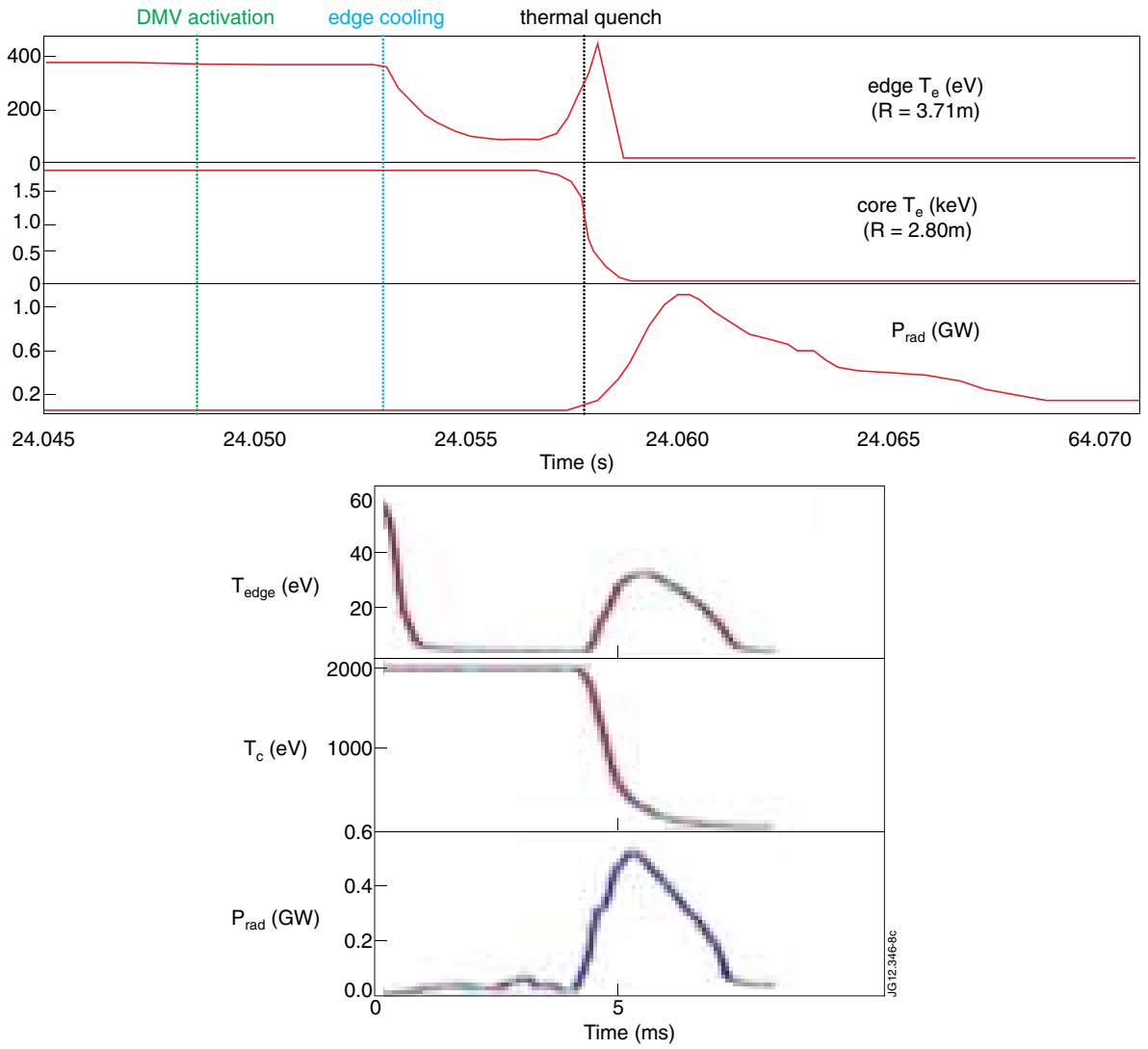


Figure 8: Comparison of time dependences for edge and core temperature and radiation power  $P_{\text{rad}}$  measured in the JET ohmic Pulse No: 76314 (upper panel) with the corresponding simulation (lower panel).

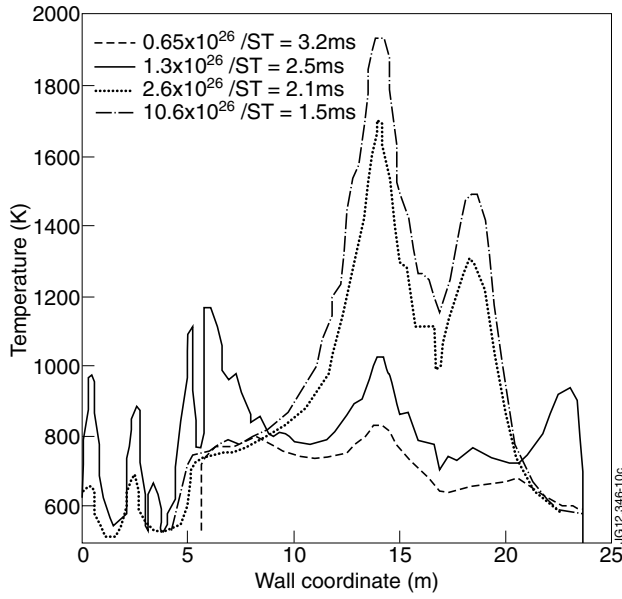


Figure 9: Radial profiles of  $T_e$  averaged over magnetic surfaces for various times during a simulated Ar MGI case in ITER at full burning plasma stored energy ( $\sim 400\text{MJ}$ ).

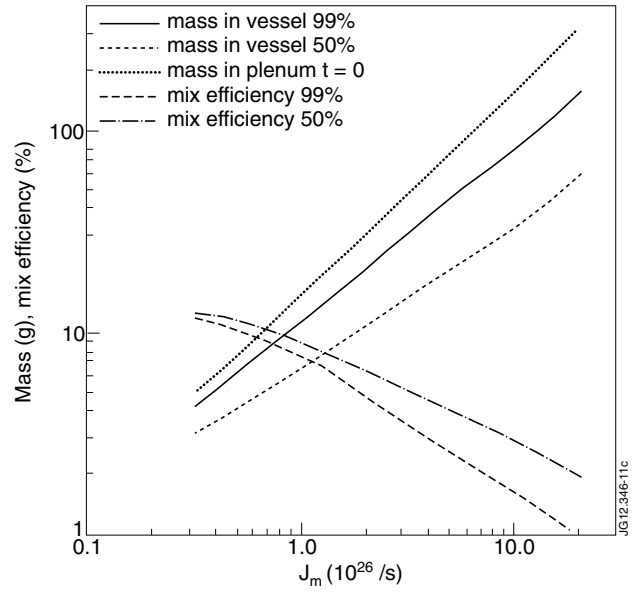


Figure 10: Poloidal surface temperature distributions as a function of gas injection rate at the instant at which  $T_{w,max}$  is reached.

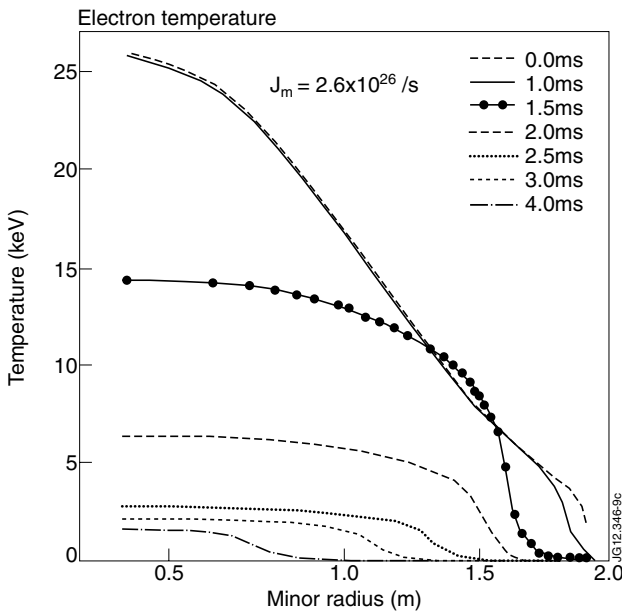


Figure 11:  $Minj$  and  $m$  as a function of  $J_m$  shown at 50% and 99% of the cooling phase with respect to radiated energy fraction.